

# Fine-structure transitions of Si and S induced by collisions with atomic hydrogen

Pei-Gen Yan \*\* and James F. Babb \*\*

Center for Astrophysics | Harvard & Smithsonian, MS 14, 60 Garden Street, Cambridge, MA 02138, USA

Accepted 2023 April 5. Received 2023 April 4; in original form 2023 March 6

#### **ABSTRACT**

Using a quantum-mechanical close-coupling method, we calculate cross-sections for fine-structure excitation and relaxation of Si and S atoms in collisions with atomic hydrogen. Rate coefficients are calculated over a range of temperatures for astrophysical applications. We determine the temperature-dependent critical densities for the relaxation of Si and S in collisions with H and compare these to the critical densities for collisions with electrons. The present calculations should be useful in modelling environments exhibiting the [S I] 25  $\mu$ m and [S I] 57  $\mu$ m far-infrared emission lines or where cooling of S and Si by collisions with H is of interest.

**Key words:** atomic process – molecular data – scattering – ISM: atoms.

## 1 INTRODUCTION

The abundances of elements are particularly important parameters for understanding the composition of the gas and dust in the interstellar medium (ISM) and the physics and chemistry behind it. Silicon and sulphur are abundant elements that are arguably less studied than, respectively, isovalent carbon and oxygen. Collisional rates for cooling of Si and S in collisions with H, such as we provide here, are useful (Hollenbach & McKee 1989) and may be efficiently calculated and presented together, similarly to complementary calculations that were given for C and O in collisions with H (e.g. Launay & Roueff 1977b and Abrahamsson, Krems & Dalgarno 2007). In the case of sulphur, observed concentrations in dense regions of the ISM appear significantly less than those in diffuse clouds (Joseph et al. 1986; Savage & Sembach 1996). Observations of sulphur fine-structure lines can assist in trying to fill this 'missing sulphur' gap. For example, the [SI] 25  $\mu$ m emission line was observed in shocked environments by Neufeld et al. (2009), Goicoechea et al. (2012), and Anderson et al. (2013) using the Spitzer Infrared Spectrograph and by Rosenthal, Bertoldi & Drapatz (2000) with the Short-Wavelength Spectrometer on the Infrared Space Observatory (ISO-SWS). In another application, recently, Betelgeuse was observed using the Echelon Cross Echelle Spectrograph on SOFIA, where the [SI]  $25 \,\mu \text{m}$  line was used to investigate circumstellar flow (Harper et al. 2020). Since emission from the sulphur atom can arise in these certain circumstellar (wind of Betelgeuse) and neutral shocked (Cshock) environments of the ISM, it is useful to have predictions of the critical densities (the densities where collisional deexcitation rates are equal to the radiative decay rates) for collisions with neutral hydrogen to reliably establish the diagnostic potential of sulphur

\* E-mail: peigen.yan@cfa.harvard.edu (P-GY); jbabb@cfa.harvard.edu

fine-structure lines at various densities and temperatures in such environments where warm atomic hydrogen is present.

In this paper, we present our calculations on the fine-structure transitions of Si and S induced by collisions with atomic hydrogen,

$$A(^{3}P_{i}) + H(^{2}S_{1/2}) \rightarrow A(^{3}P_{i'}) + H(^{2}S_{1/2}),$$
 (1)

where A can be Si or S and j and j' can be 0, 1, or 2, respectively. In collisions with H, there is little theoretical work on the Si and S systems, compared to C and O where fully quantum calculations are available. Semiclassically calculated rate coefficients were given by Bahcall & Wolf (1968, equation 42), Tielens & Hollenbach (1985, table 4), and Hollenbach & McKee (1989, table 8). The present rate coefficients obtained from fully quantum calculated cross-sections could be used for modelling or simulation and other astrophysical applications.

# 2 THEORETICAL MODELS

The quantum-mechanical application of scattering theory to fine-structure changing collisions has a long history (see e.g. Launay & Roueff 1977a, 1977b; Roueff 1990; Flower, Bourhis & Launay 2000, and references therein). Our approach is detailed in Yan & Babb (2022, 2023b). Here, we give a brief summary to provide specific information for the present calculations. The fine-structure splitting energies  $\varepsilon_{j_a}$  are adopted from NIST (Kramida et al. 2022), where for Si  $(j_a=0,1,2)$ 

$$\varepsilon_0 = 0, \qquad \varepsilon_1 = 77.115 \text{ cm}^{-1}, \qquad \varepsilon_2 = 223.157 \text{ cm}^{-1}, \qquad (2)$$

and for S  $(j_a = 2, 1, 0)$ 

$$\varepsilon_2 = 0, \qquad \varepsilon_1 = 396.055 \text{ cm}^{-1}, \qquad \varepsilon_0 = 573.640 \text{ cm}^{-1}.$$
 (3)

The cross-sections for fine-structure transitions are given by

$$\sigma_{j_a \to j_a'}(E) = \sum_J \frac{\pi}{k_{j_a}^2} \frac{2J+1}{(2j_a+1)(2j_b+1)} \sum_{j_{ab}lj_{ab}'l_{bb}'} |T_{j_a'j_{ab}'l';j_aj_{ab}l}^J|^2, \quad (4)$$

© The Author(s) 2023.

Published by Oxford University Press on behalf of Royal Astronomical Society. This is an Open Access article distributed under the terms of the Creative Commons Attribution License (http://creativecommons.org/licenses/by/4.0/), which permits unrestricted reuse, distribution, and reproduction in any medium, provided the original work is properly cited.

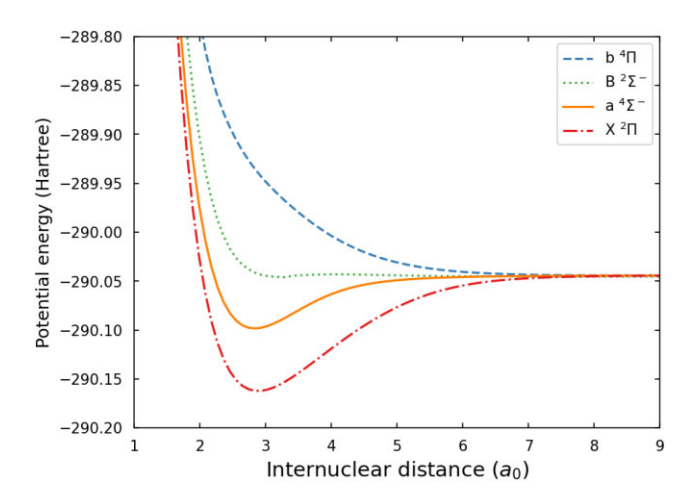
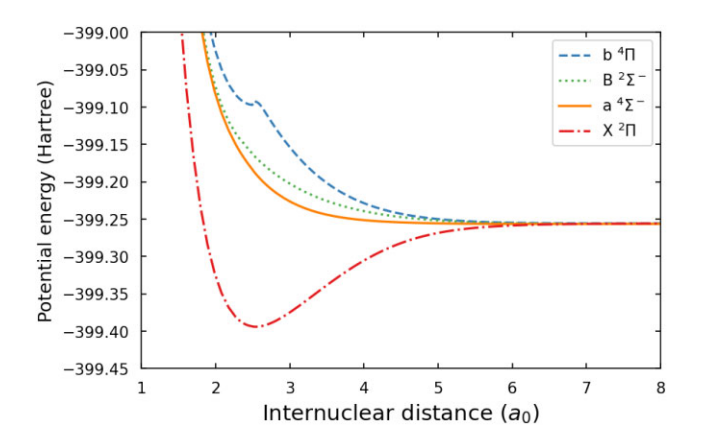


Figure 1. Potential energies for the SiH system as functions of the internuclear distance R, labelled from the top down:  $b^4\Pi$  (blue dashed line),  $B^2\Sigma^-$  (green dotted line),  $a^4\Sigma^-$  (orange solid line), and  $X^2\Pi$  (red dash–dotted line).

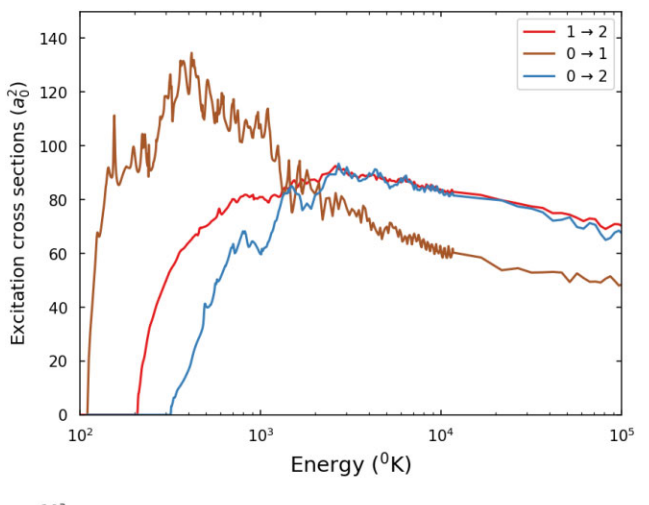


**Figure 2.** Potential energies for the SH system as functions of the internuclear distance R, labelled from the top down:  $b^4\Pi$  (blue dashed line),  $B^2\Sigma^-$  (green dotted line),  $a^4\Sigma^-$  (orange solid line), and  $X^2\Pi$  (red dash-dotted line).

where  $\sigma^J_{j_a \to j_a'}(E)$  are the partial cross-sections,  $k_{j_a}$  is the wavenumber defined by  $k_{j_a}^2 = 2\mu(E - \varepsilon_{j_a})$ ,  $\mu$  is the reduced mass of systems a and b, E is the total collision energy, and  $\varepsilon_{j_a}$  is the fine-structure state splitting energy of the Si or S atom. The T matrix is defined by  $T^J = -2iK^J(I - iK^J)^{-1}$ , where  $K^J$  is the open channel reaction matrix defined in Johnson (1973). To solve for the radial wavefunctions, which determine the scattering matrices, we used the quantum close-coupling formalism with the wavefunctions expanded in the space-fixed basis (Yan & Babb 2022, 2023b).

# 3 INTERATOMIC POTENTIALS

For both  $\mathrm{Si}(^3P)$  and  $\mathrm{S}(^3P)$ , the electronic states involved in the fine-structure transitions with  $\mathrm{H}(^2S)$  are the  $\mathrm{b}^4\Pi$ ,  $\mathrm{B}^2\Sigma^-$ ,  $\mathrm{a}^4\Sigma^-$ , and  $\mathrm{X}^2\Pi$  states. The potentials for SiH and SH were obtained by using the multireference configuration interaction Douglas–Kroll–Hess (MRCI-DKH) method with the augmented-correlation-consistent polarized valence 5-tuple zeta (aug-cc-pV5Z-dk) basis within MOLPRO 2010.1 (Werner et al. 2010) in the  $C_{2v}$  Abelian symmetry point group. For both SiH and SH, these potentials were calculated for internuclear distances R from 1.13 to 9.07  $a_0$  at an interval of 0.095  $a_0$  and from 9.07 to 10.4  $a_0$  at an interval of 0.19  $a_0$ . Note that



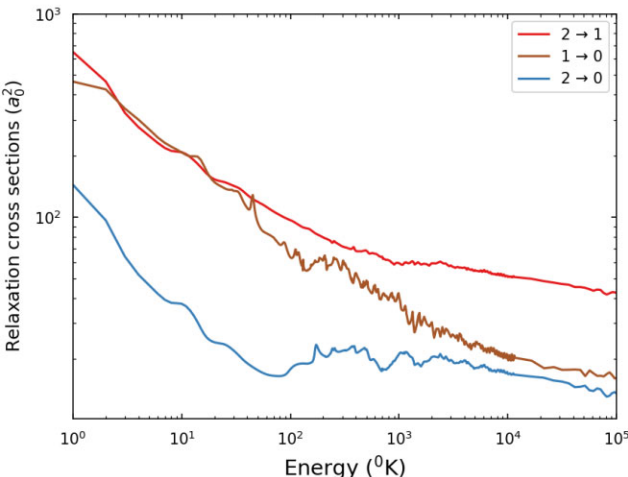


**Figure 3.** Excitation and relaxation cross-sections for fine-structure transitions of Si in collision with H. The three transitions  $(j \to j')$  are labelled with different colours.

we have given the values of R in units of  $a_0$ , because the scattering calculations were carried out in atomic units (a.u.) (1  $a_0 \approx 0.529 \text{ Å}$ ).

For the SiH system, 10 molecular orbitals (MOs) are used for the active space: 6  $a_1$ , 2  $b_1$ , and 2  $b_2$  symmetry MOs. The remaining five electrons are put in the closed-shell orbitals. The potentials calculated from MOLPRO are shown in Fig. 1. Our calculated potentials are in good agreement with Zhang et al. (2018); for example, for the  $X^2\Pi$  state we find  $D_e=3.210\,\mathrm{eV}$  at  $R_e=1.524\,\mathrm{Å}$  compared to their value of  $D_e=3.193\,\mathrm{eV}$  at  $R_e=1.517\,\mathrm{Å}$ .

For the SH system, 12 MOs are used for the active space: 6  $a_1$ , 3  $b_1$ , and 3  $b_2$  symmetry MOs. The remaining five electrons are put in the closed-shell orbitals. The potentials calculated from MOLPRO are shown in Fig. 2. Our calculated potentials are in accordance with those of Hirst & Guest (1982). For the  $X^2\Pi$  state, our value of  $D_e = 3.77 \, \text{eV}$  agrees with the value 3.791 eV adopted by Császár, Leininger & Burcat (2003) and Gorman, Yurchenko & Tennyson (2019).

In order to have the potentials correlate asymptotically to the separated atom limits, which are taken to be the reference energies for the scattering calculations, the potentials for SiH and SH as shown in Figs 1 and 2 were shifted in energy and joined at  $R=9.83\,a_0$  to the long-range form  $-C_6/R^6$ . Smooth fits were obtained using estimates of  $C_6$  from Gould & Bučko 2016; the values used were  $C_6=44.1$ 

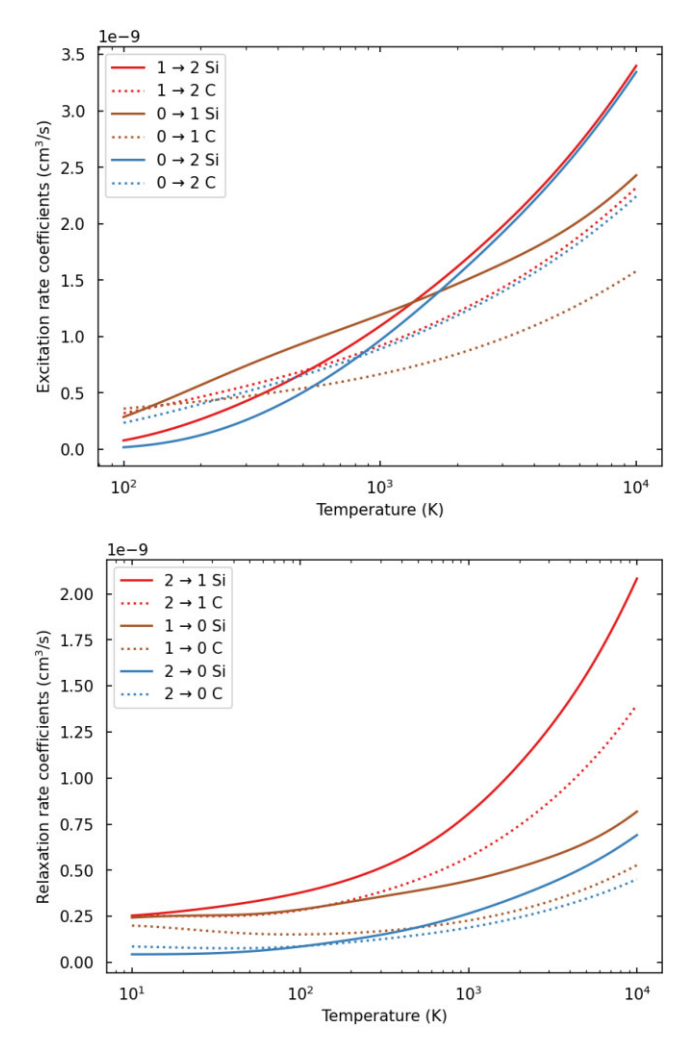


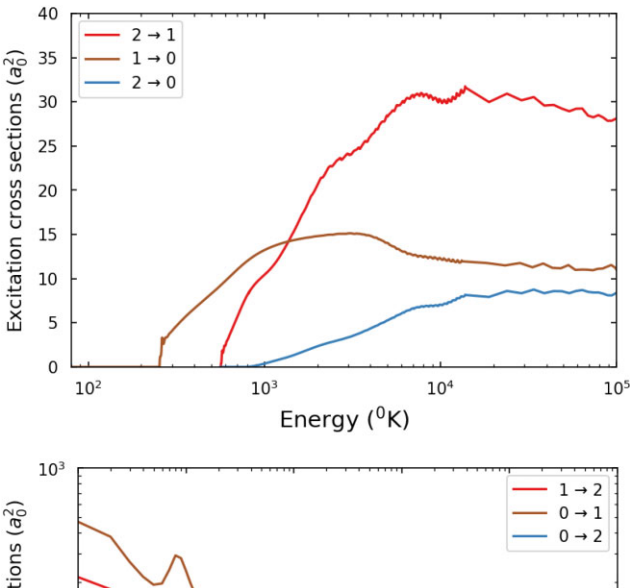
**Figure 4.** Excitation and relaxation rate coefficients for fine-structure transitions of Si in collision with H (solid lines), this work, and for C in collision with H (dotted lines) from Yan & Babb (2023b). The three transitions  $(j \rightarrow j')$  are labelled with different colours.

**Table 1.** Rate coefficients (in units of  $10^{-9} \text{ cm}^3 \text{s}^{-1}$ ) for the fine-structure excitation and relaxation of  $\text{Si}(^3P_i)$  by H.

T(K)	$j = 0 \rightarrow j' = 1$	$j = 0 \to j' = 2$	$j = 1 \rightarrow j' = 2$
100	0.280	0.017	0.076
200	0.556	0.122	0.260
500	0.917	0.493	0.657
700	1.037	0.695	0.843
1000	1.163	0.943	1.067
2000	1.433	1.505	1.580
5000	1.867	2.395	2.440
7000	2.084	2.793	2.838
10 000	2.374	3.271	3.323
T(K)	$j=1 \rightarrow j'=0$	$j = 2 \rightarrow j' = 0$	$j=2 \rightarrow j'=1$
10	0.238	0.043	0.248
20	0.247	0.044	0.272
50	0.255	0.058	0.319
70	0.265	0.069	0.342
100	0.280	0.084	0.370
200	0.322	0.120	0.443
500	0.381	0.186	0.598
700	0.405	0.219	0.682
1000	0.433	0.259	0.788

Table 1 - continued

T(K)	$j = 0 \rightarrow j' = 1$	$j = 0 \rightarrow j' = 2$	$j=1 \to j'=2$
2000	0.505	0.353	1.052
5000	0.636	0.510	1.526
7000	0.705	0.584	1.754
10 000	0.800	0.675	2.036



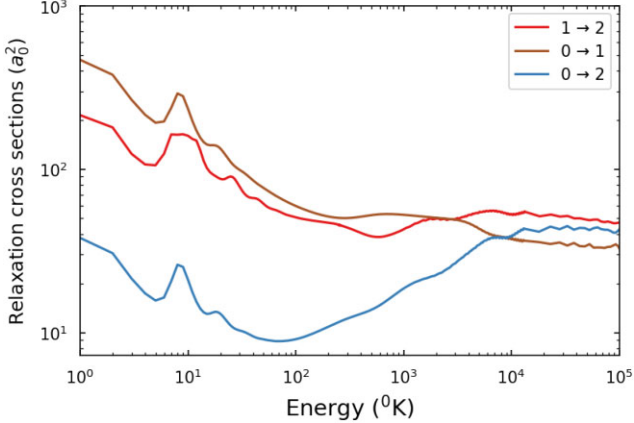


**Figure 5.** Excitation and relaxation cross-sections for fine-structure transitions of S in collision with H. The three transitions  $(j \to j')$  are labelled with different colours.

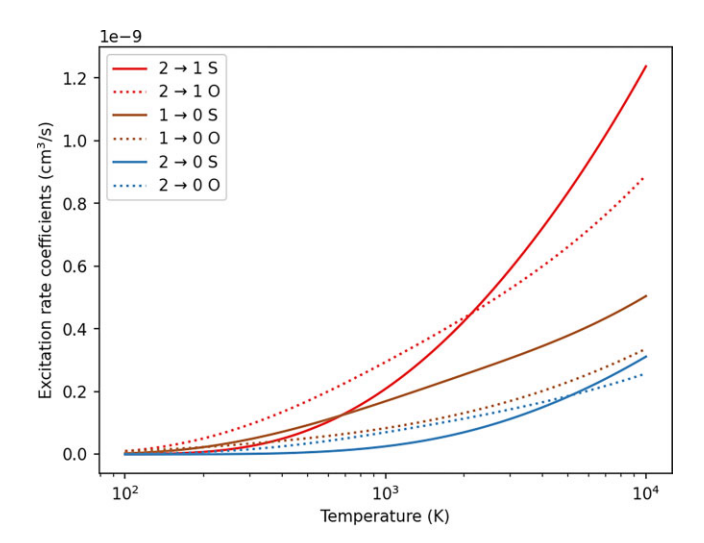
a.u. between  $Si(^3P)$  and  $H(^2S)$  and  $C_6=30.1$  a.u. between  $S(^3P)$  and  $H(^2S)$ .

### 4 RESULTS

Rate coefficients as functions of temperature are obtained by averaging the cross-sections over a Maxwellian energy distribution,

$$k_{j_a \to j_a'}(T) = \left(\frac{8}{\pi \mu k_B^3 T^3}\right)^{1/2} \int_0^\infty \sigma_{j_a \to j_a'}(E_k) e^{-E_k/k_B T} E_k dE_k,$$
 (5)

where T is the temperature,  $k_{\rm B}$  is the Boltzmann constant, and  $E_{\rm k}$  is the kinetic energy. The scattering equations were integrated from  $R=1.2\,a_0$  to  $R=30\,a_0$ . Over this range, accordingly the potentials were utilized as described in Section 3 with the potential values for  $R<9.83\,a_0$  interpolated using cubic splines. Cross-sections were calculated using equation (4) from threshold, equations (2) and (3), to sufficiently high collisional energies ( $10^5\,{\rm K}$  or about  $8.62\,{\rm eV}$ ) to ensure that the integration in equation (5) could be accurately



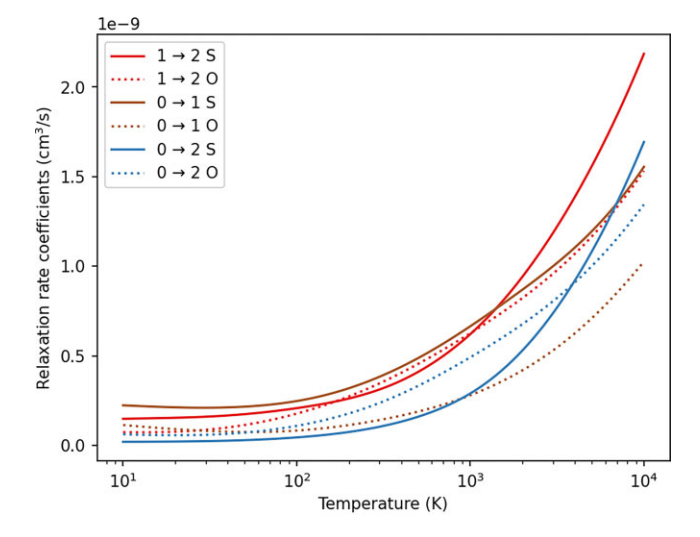


**Figure 6.** Excitation and relaxation rate coefficients for fine-structure transitions of S in collision with H (solid lines), this work, and for O in collision with H (dotted lines), from Yan & Babb (2022). The three transitions  $(j \rightarrow j')$  are labelled with different colours.

evaluated up to temperatures of  $10\,000$  K. [Note that the Si( $^1D$ )–H and S( $^1D$ )–H channels, respectively, open at about 0.8 and 1.2 eV. Our cross-sections do not include atomic Si or S electronic excitations higher than the ground  $^3P$  terms].

In Fig. 3, we present our calculated excitation and relaxation cross-sections of the fine-structure transitions for the Si–H system. The corresponding rate coefficients are given in Fig. 4 and in Table 1. In Fig. 4, we also show the fine-structure excitation and relaxation rate coefficients for the C–H system (Yan & Babb 2023b) for the purpose of comparison. Because Si and C are isovalent and share the same fine-structure level ordering with  $j_a$ , the relaxation cross-sections for Si and H collisions, equation (2), are similar to those for C and H (dotted lines) (Yan & Babb 2023b), though we find the Si–H values are larger than the C–H values for relatively high energy T > 1000 K. Also, we find that the  $0 \rightarrow 1$  excitation rate coefficients for Si and H collisions are much larger than those for C and H collisions.

For the S atom in collision with H, the excitation and relaxation cross-sections for the fine-structure transitions as functions of energy are shown in Fig. 5, where we find that the cross-sections for

**Table 2.** Rate coefficients (in units of  $10^{-9}$  cm<sup>3</sup>s<sup>-1</sup>) for the fine-structure excitation and relaxation of  $S(^3P_i)$  by H.

T(K)	$j = 1 \rightarrow j' = 0$	$j=2 \to j'=0$	$j = 2 \rightarrow j' = 1$
100	0.003	_	_
200	0.023	_	0.008
500	0.091	0.006	0.076
700	0.126	0.013	0.130
1000	0.167	0.025	0.207
2000	0.250	0.070	0.420
5000	0.369	0.178	0.813
7000	0.422	0.235	0.991
10 000	0.492	0.304	1.204
T(K)	$j = 0 \rightarrow j' = 1$	$j = 0 \rightarrow j' = 2$	$j = 1 \rightarrow j' = 2$
10	0.224	0.020	0.149
20	0.212	0.022	0.154
50	0.216	0.029	0.174
70	0.227	0.035	0.189
100	0.248	0.045	0.208
200	0.319	0.075	0.262
500	0.487	0.160	0.410
700	0.569	0.213	0.500
1000	0.665	0.290	0.621
2000	0.870	0.531	0.942
5000	1.194	1.080	1.557
7000	1.351	1.355	1.841
10 000	1.554	1.693	2.185

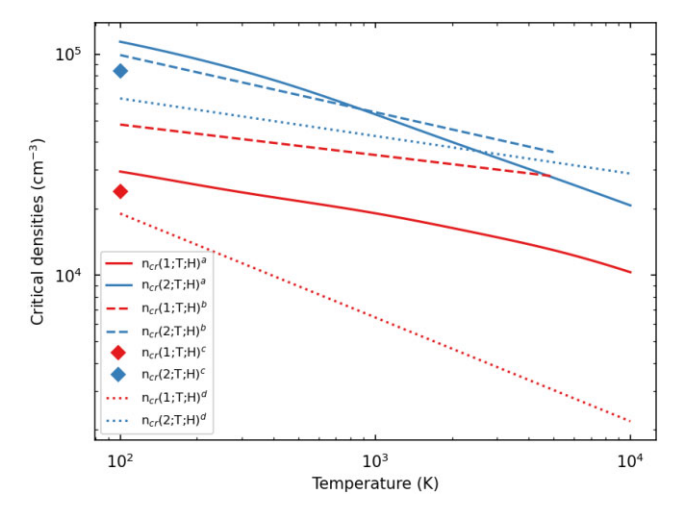


**Figure 7.** For relaxation collisions of Si with H, comparison of critical densities of the present full quantum close-coupling calculations (a solid lines) with those of Draine (2011, table 17.1) (b dashed lines), with those of Tielens & Hollenbach (1985, table 4) (c diamond marker), and with those of semiclassical calculations from Hollenbach & McKee (1989, table 8) (d dotted lines), where blue denotes the ( $2 \rightarrow 1$ ) transition and red denotes the ( $1 \rightarrow 0$ ) transition. Note that the ( $2 \rightarrow 0$ ) transition is forbidden (Hollenbach & McKee 1989).

relaxation for S and H show some resonances for collisional energies around 10 K. The corresponding rate coefficients are given in Fig. 6 and Table 2. In Fig. 6, we also show our calculations on fine-structure excitation and relaxation rate coefficients for the O–H system (Yan & Babb 2022) for the purpose of comparison. We find that the excitation rate coefficients for S and H are similar to those of O and H. However, the  $0 \rightarrow 1$  relaxation rate coefficient for S and H is also much larger than that for O and H.

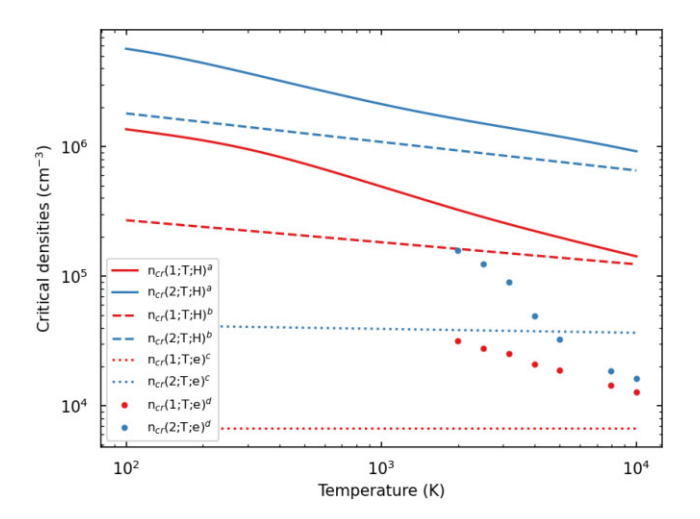


**Figure 8.** For relaxation collisions of S with H and with electrons, a solid lines are the present full quantum close-coupling calculations for critical densities of the relaxation of S in collision with hydrogen and b dashed lines are the semiclassical calculations for critical densities of the relaxation in S–H collisions from Hollenbach & McKee (1989, table 8). For relaxation in S–electron collisions, c small dotted lines are the critical densities from Hollenbach & McKee (1989) and d large dotted lines are the critical densities calculated using the quantum R-MATRIX calculations of Tayal (2004). The blue denotes the  $(1 \rightarrow 2)$  transition and red denotes the  $(0 \rightarrow 1)$  transition. Note that the  $(2 \rightarrow 0)$  transition is forbidden (Hollenbach & McKee 1989).

From Figs 3–6, we can find that the cross-sections and rate coefficients of Si in collision with H are relatively larger than those of S in collision with H, which are caused by the more 'attractive' (deeper) potentials of SiH compared to SH (the  $a^4\Sigma^-$  electronic state of SiH has numerous bound ro-vibrational levels, while that of SH is repulsive). The present calculations for Si in collision with H and for S in collision with H can replace rate coefficients estimated by scaling values for Si in collision with He and for S in collision with He values (Lique, Kłos & Le Picard 2018).

The critical density  $n_c$  is defined as

$$n_{c}(j;T;x) = \frac{\sum_{j'} A(j \to j')}{\sum_{j'} k_{j \to j'}(T;x)},$$
(6)

where  $A(j \rightarrow j')$  is the transition probability (Mendoza 1983) and  $k_{j \rightarrow j'}(T;x)$  is the relaxation rate coefficient for collisions with species x, which may be hydrogen atoms (H) or electrons (e). For the collisions of Si with H, the present calculations of critical densities are shown in Fig. 7 along with the values from Draine (2011, table 17.1) and from Tielens & Hollenbach (1985). For the collisions of S with H, the present calculations are shown in Fig. 8 along with the semiclassical calculations of Hollenbach & McKee (1989). In Fig. 8, we also present the critical densities for the relaxation of S in collisions with electrons, which we evaluated using the quantum R-MATRIX effective collision strengths from Tayal (2004); for comparison, we also include the the semiclassical calculations of Hollenbach & McKee (1989).

## 5 CONCLUSION

Fine-structure excitation and relaxation cross-sections and rate coefficients for the Si and S atoms in collision with atomic hydrogen are obtained by using quantum-mechanical close-coupling methods. The electronic potential curves of SiH and SH are obtained by using

the MRCI-DKH method. The critical densities for the Si and S atoms in H collisions and their comparisons with other calculations or with electron collisions are also given. The present calculations may be useful in diagnostics of astrophysical environments such as shocked and circumstellar environments.

#### ACKNOWLEDGEMENTS

This work was supported by NASA APRA grant no. 80NSSC19K0698.

### DATA AVAILABILITY

The rates for collisional relaxation by H presented in Table 1 for Si and in Table 2 for S are given in LAMDA format (Schöier et al. 2005) at Figshare (Yan & Babb 2023a).

### REFERENCES

Abrahamsson E., Krems R. V., Dalgarno A., 2007, ApJ, 654, 1171 Anderson D. E., Bergin E. A., Maret S., Wakelam V., 2013, ApJ, 779, 141 Bahcall J. N., Wolf R. A., 1968, ApJ, 152, 701

Császár A. G., Leininger M. L., Burcat A., 2003, J. Phys. Chem. A, 107, 2061Draine B. T., 2011, Physics of the Interstellar and Intergalactic Medium.Princeton Univ. Press, Princeton, NJ

Flower D., Bourhis G., Launay J.-M., 2000, Comput. Phys. Commun., 131, 187

Goicoechea J. R. et al., 2012, A&A, 548, A77

Gorman M. N., Yurchenko S. N., Tennyson J., 2019, MNRAS, 490, 1652

Gould T., Bučko T., 2016, J. Chem. Theory Comput., 12, 3603

Harper G. M., DeWitt C. N., Richter M. J., Guinan E. F., Wasatonic R., Ryde N., Montiel E. J., Townsend A. J., 2020, ApJ, 893, L23

Hirst D., Guest M., 1982, Mol. Phys., 46, 427

Hollenbach D., McKee C. F., 1989, ApJ, 342, 306

Johnson B., 1973, J. Comput. Phys., 13, 445

Joseph C. L., Snow T. P., Jr, Seab C. G., Crutcher R. M., 1986, ApJ, 309, 771
Kramida A., Ralchenko Y., Reader J., and NIST ASD Team, 2022, NIST
Atomic Spectra Database (ver. 5.10), [Online]. Available at https://physics.nist.gov/asd [accessed Jan 30]. National Institute of Standards and Technology, Gaithersburg, MD

Launay J. M., Roueff E., 1977a, J. Phys. B: At. Mol. Phys., 10, 879

Launay J. M., Roueff E., 1977b, A&A, 56, 289

Lique F., Kłos J., Le Picard S. D., 2018, Phys. Chem. Chem. Phys., 20, 5427Mendoza C., 1983, in Flower D. R., ed., Proc. IAU Symp. 103, Planetary Nebulae. D. Reidel Publishing Co., Dordrecht, p. 143

Neufeld D. A. et al., 2009, ApJ, 706, 170

Rosenthal D., Bertoldi F., Drapatz S., 2000, A&A, 356, 705

Roueff E., 1990, A&A, 234, 567

Savage B. D., Sembach K. R., 1996, ApJ, 470, 893

Schöier F. L., van der Tak F. F. S., van Dishoeck E. F., Black J. H., 2005, A&A, 432, 369

Tayal S. S., 2004, ApJS, 153, 581

Tielens A. G. G. M., Hollenbach D., 1985, ApJ, 291, 722

Werner H.-J. et al., 2010, Molpro, version 2010.1, a package of ab initio programs, https://www.molpro.net

Yan P.-G., Babb J. F., 2022, Res. Notes Am. Astron. Soc., 6, 145

Yan P.-G., Babb J. F., 2023a, Available at Figshare: https://doi.org/10.6084/m9.figshare.22223284

Yan P.-G., Babb J. F., 2023b, MNRAS, 518, 6004

Zhang Y.-G., Dou G., Qi J.-X., Cui J., 2018, Comput. Theor. Chem., 1134, 8

This paper has been typeset from a TEX/LATEX file prepared by the author.